

AN INTEGRAL AND TIME-VARYING SLIDING MODE SPEED CONTROL OF SWITCHED RELUCTANCE MOTOR DRIVES

CUNHE LI, GUOFENG WANG*, YUNSHENG FAN AND YAN LI

College of Information Science and Technology
Dalian Maritime University
No. 1, Linghai Road, Dalian 116026, P. R. China
*Corresponding author: gfwangsh@163.com

Received August 2016; accepted November 2016

ABSTRACT. *An integral and time-varying sliding mode speed controller (ITSMC) is designed to improve the dynamic performance and robustness of switched reluctance motor (SRM) drive. The integral of the speed error signal is introduced into sliding surface in this design to enhance the accuracy of system control. And the time-varying term is introduced to improve the convergence speed of the sliding surface. In order to further improve robustness and chattering of the system, a load disturbance estimator using an Luenberger observer is proposed to estimate the change of the load torque. Comparative studies are carried out between the proposed control scheme and the traditional PI control, and the simulation results demonstrate that the proposed control scheme can improve dynamic response performance and enhance the robustness of SRM drive system.*

Keywords: SRM, Speed control, ITSMC, Luenberger observer, Load disturbance

1. **Introduction.** Switched reluctance motor (SRM) has been widely used in various industry fields because of its simple structure, low-cost, large starting torque, wider speed range and high efficiency [1,2]. However, the nonlinear inductance of the SRM makes the electromagnetic torque highly nonlinear and difficult to control. Moreover, in industrial applications, the parameters variations and external load disturbance also have a great influence on the speed control of the SRM.

In recent years, feedback linearization control [3], adaptive control [4], model predictive control [5], fuzzy control [6], neural network control [7] and sliding mode variable structure control [8] have been applied to the SRM drive system. The main advantage of sliding mode control is that, once the system state reaches a sliding surface, the system dynamics remain insensitive to a class of parameter uncertainties and disturbances. A sliding mode variable structure control for SRM speed control system is developed in [9]. A hybrid control scheme was implemented by using integral variable structure control and neural network compensation control for SRM drives in [10]. In [11], a nonsingular fast terminal sliding mode controller based on state was designed for SRM positioning control. A time-varying sliding mode control approach is presented to improve the dynamic performance of the system in [12].

In this paper, an integral and time-varying sliding mode speed controller (ITSMC) is proposed to improve the dynamic performance and robustness of SRM drive. The main advantages of the proposed controller are that: (1) the exponential time-varying term is introduced to improve the dynamic performance of the SRM drive system; (2) the load disturbance observer is designed to observe the change of the load and the observed load torque is integrated into the design of the ITSMC, which can better suppress the chattering of the controller. At last the correctness and robustness of the proposed control algorithm are verified through simulation. This paper is organized as follows. Section 2 presents the operation principle and mathematical model of SRM. In Section 3, the ITSMC is

designed. The simulation for the proposed control scheme is presented in Section 4. And Section 5 contains conclusions.

2. **SRM.** SRM has unique double salient poles on the stator and rotor. The opposite stator poles are supplied by a converter phase, and the phase current is switched on and off in synchronism with the rotor position. SRM motions follow the minimum reluctance principle. Figure 1 shows a three-phase, 6/4 poles SRM and its power converter.

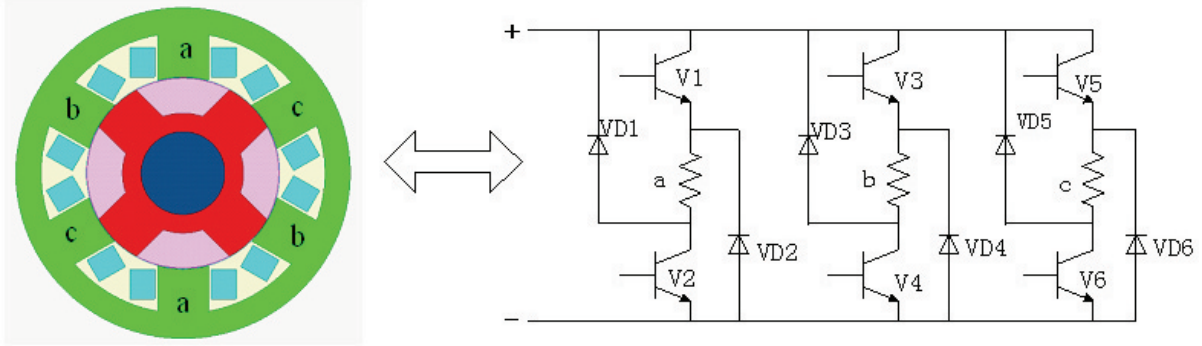


FIGURE 1. SRM with power converter

The mathematical model of the SRM can be described as

$$\begin{cases} u_j = R_j i_j + \frac{d\psi_j(\theta, i_j)}{dt}, & j = a, b, c \\ T_j = \frac{dW_c(\theta, i)}{d\theta} \Big|_{i_j=const} = -\frac{dW_s(\theta, i)}{d\theta} \Big|_{\psi_j=const} \end{cases} \quad \begin{cases} T_e = \sum_{j=1}^m T_j(i_j, \theta) \\ T_e = J \frac{d\omega_r}{dt} + k_\omega \omega_r + T_L \end{cases} \quad (1)$$

where u_j and R_j are the voltage and the resistance of the j th stator phase, respectively. i_j and ψ_j are the current and the flux linkage of the j th stator phase, respectively. θ is the current rotor angle position. T_j is the electromagnetic torque of phase j , $W_c = \int_0^i \psi(i, \theta) di$ is the coenergy, and $W_s = \int_0^\psi i(\psi, \theta) d\psi$ is the stored field energy. T_e is the electromagnetic torque. ω_r is the rotor speed, T_L is the external load, k_ω is the frictional coefficient, and J is the moment of inertia.

3. **ITSMC Design.** In this section, a double closed loop drive system of speed control and torque control is developed for SRM. An ITSMC is used to control the motor speed in the outer loop and the direct instantaneous torque control (DITC) method is applied to the inner loop to achieve the tracking of torque.

3.1. **Speed controller.** Define the state variable of SRM drive system as follows:

$$x_1 = \omega_r^* - \omega_r, \quad x_2 = \int_0^t x_1(\tau) d\tau = \int_0^t (\omega_r^* - \omega_r) dt \quad (2)$$

where ω_r^* and ω_r are reference speed and actual speed, respectively.

Considering (2) and differentiating x_1 and x_2 , we have

$$\dot{x}_1 = -k_\omega x_1/J - u/J + (T_L + k_\omega \omega_r^*)/J, \quad \dot{x}_2 = x_1 \quad (3)$$

where $u = T_e$ is the output variable of controller.

In the real application, the parameters change when the drive system is operated under different conditions. Considering the uncertainty of model, (3) can be rewritten as

$$\begin{aligned} \dot{x}_1 &= (-k_\omega x_1 - u + T_L + k_\omega \omega_r^*)/J \\ &= (-k_\omega/J + \Delta_1)(x_1 + \omega_r^*) + (-1/J + \Delta_2)(u - T_L) \\ &= Ax_1 + bu - bT_L + d_L \end{aligned} \quad (4)$$

where $d_L = -k_\omega \omega_r^*/J + \Delta_1(x_1 + \omega_r^*) + \Delta_2(u - T_L)$ defines the internal disturbance of system, $A = -k_\omega/J$, $b = -1/J$.

The integral term $\int_0^t x_1(\tau)d\tau$ of the state is introduced into the sliding surface to eliminate or reduce steady-state error and the time-varying term $\nu(t)$ is introduced to improve the speed of convergence effectively. The sliding surface function with integral term and time-varying term can be expressed as

$$s(x_1, x_2, t) = x_1 + cx_2 + \nu(t) \tag{5}$$

where c is a constant that satisfies the Hurwitz condition, $\nu(t) = me^{-t/n}$ satisfies $\nu(t) \rightarrow 0$ as $t \rightarrow \infty$, $m > 0$ and $n > 0$ are design parameters.

In order to realize the global robustness of sliding mode control, the phase trajectory of the system needs to be in a time varying sliding surface at the initial time. Let $s = 0$, and we have

$$m = -x_1(0) - c \int_0^t x_1(0) \tag{6}$$

To improve dynamic quality of drive system, the exponential reaching law is adopted

$$\dot{s} = -\varepsilon \text{sgn}(s) - ks \tag{7}$$

where $\varepsilon > 0$ and $k > 0$ are the design parameters, and $\text{sgn}(\cdot)$ denotes the sign function.

The time derivative of (5) is

$$\dot{s} = \dot{x}_1 + cx_1 - me^{-t/n}/n = -\varepsilon \text{sgn}(s) - ks \tag{8}$$

Substituting (4) into (8), the control law is designed as

$$u = -[(A + c)x_1 - me^{-t/n}/n - bT_L + \varepsilon \text{sgn}(s) + ks]/b \tag{9}$$

From (9), it can be found that T_L has an important effect on the control performance. However, it is difficult to measure in practical application. To overcome this problem, an ITSMC with the load disturbance observer is presented in Section 3.2.

3.2. Load disturbance observer. The inaccessible load torque T_L can be assumed as an unknown constant. By $dT_L/dt = 0$ and (1), the system equation for a disturbance torque observer can be expressed as follows

$$\dot{\zeta} = \bar{A}\zeta + \bar{b}u, \quad \eta = \bar{C}\zeta \tag{10}$$

where $\zeta = [\omega \ T_L]^T$ is state vector. $u = T_e$ and $\eta = \omega$ are input variable and output variable, respectively. $\bar{b} = [1/J \ 0]^T$, $\bar{C} = [1 \ 0]$ and $\bar{A} = \begin{bmatrix} -k_\omega/J & -1/J \\ 0 & 0 \end{bmatrix}$ are constant matrices.

For this system, (\bar{A}, \bar{C}) is observable. A full order Luenberger observer can be designed as

$$\dot{\hat{\zeta}} = \bar{A}\hat{\zeta} + \bar{b}u + H(\eta - \hat{\eta}), \quad \hat{\eta} = \bar{C}\hat{\zeta} \tag{11}$$

where $\hat{\zeta} = [\hat{\omega} \ \hat{T}_L]^T$ is the observed value of ζ , $\hat{\eta}$ is observed value of η and $H = [h_1 \ h_2]^T$ is the output feedback gain matrix.

Error equation of observer can be expressed as

$$\dot{\zeta} - \dot{\hat{\zeta}} = (\bar{A} - H\bar{C}) (\zeta - \hat{\zeta}) \tag{12}$$

and the solution is

$$\zeta(t) - \hat{\zeta}(t) = e^{(\bar{A}-H\bar{C})(t-t_0)} [\zeta(t_0) - \hat{\zeta}(t_0)] \tag{13}$$

From (13) it can be seen that as long as all the eigenvalues of the matrix $(\bar{A} - H\bar{C})$ have negative real parts, the initial state vector error always will gradually close to zero according to the exponential decay rule. And the decay rate depends on the pole assignment of the matrix $(\bar{A} - H\bar{C})$. According to the output feedback theorem [13], if

the controlled object can be observed the poles can be arbitrarily configured. Thus, the existence of the state observer is guaranteed.

Substituting the estimate value \hat{T}_L into (9), the control law can be rewritten as

$$u = -[(A + c)x_1 - me^{-t/n}/n - b\hat{T}_L + \varepsilon \text{sgn}(s, \delta) + ks]/b \quad (14)$$

3.3. Stability analysis. We are now in a position to prove the stability of ITSMC.

Assumption 1. *The uncertainty term $f = d_L + \tilde{T}_L$ of the system is bounded satisfying $|f| \leq \rho$ with $\rho > 0$, a positive constant, where $\tilde{T}_L = \hat{T}_L - T_L$ is the estimate error.*

Theorem 3.1. *Consider the SRM drive system (4) with **Assumption 1** and the sliding surface function (5). If the control law is chosen as (14) and ε meets $\varepsilon > \rho$, then the system is asymptotically stable.*

Proof: The time derivative of sliding surface function can be described as

$$\dot{s} = \dot{x}_1 + cx_1 - me^{-t/n}/n = Ax_1 + bu - bT_L + d_L + cx_1 - me^{-t/n}/n \quad (15)$$

Consider the Lyapunov function candidate as $V(t) = s^2/2$ and derivative of $V(t)$ is

$$\dot{V}(t) = s\dot{s} = s[Ax_1 + bu - bT_L + d_L + cx_1 - me^{-t/n}/n] \quad (16)$$

When $s > 0$, substituting (14) into (16), we have

$$\begin{aligned} \dot{V}(t) &= s[Ax_1 + bu - bT_L + d_L + cx_1 - me^{-t/n}/n] \\ &= s[Ax_1 - (A + c)x_1 + me^{-t/n}/n + b\hat{T}_L - \varepsilon \\ &\quad - ks - bT_L + d_L + cx_1 - me^{-t/n}/n] \\ &= -ks^2 + s[f - \varepsilon] \leq -ks^2 + s[\rho - \varepsilon] < 0 \end{aligned} \quad (17)$$

When $s < 0$, $\dot{V}(t) = s\dot{s} < 0$ can be also proved in the same way.

According to Lyapunov's stability theory, the system is asymptotically stable.

Theorem 3.1 has been proved.

From (17), it can be seen that the estimate value \hat{T}_L of load torque as a known variable exists in the control law. The values of design parameters ε are greatly reduced which are only greater than the sum of the internal disturbance and the estimate error of external load disturbance. Thus, an integral and time-varying sliding control method based on the load disturbance observer not only can overcome the effect of load disturbance on the system control performance, but can reduce the sliding mode control gain, weaken the chattering of the sliding mode control system. In addition, to further suppress the chattering phenomena, we use the saturation function $\text{sat}(s, \delta)$ instead of the sign function $\text{sgn}(s)$. The saturation function $\text{sat}(s, \delta)$ can be expressed as follows

$$\text{sat}(s, \delta) = \begin{cases} 1, & s \geq \delta \\ s/\delta, & |s| < \delta \\ -1, & s \leq -\delta \end{cases} \quad (18)$$

where the constant factor $\delta > 0$ defines the thickness of the boundary layer.

The signum function $\text{sgn}(s)$ in the control law (14) is replaced by a saturation function $\text{sat}(s, \delta)$, and the actual control law (14) can be rewritten as

$$u = -[(A + c)x_1 - me^{-t/n}/n - bT_L + \varepsilon \text{sat}(s, \delta) + ks]/b \quad (19)$$

3.4. Torque control method. In order to minimize the torque ripple, the DITC method is applied in the drive system inner loop. Based on the rotor position and the torque error, the output signal can be determined to control the work of the power converter, and then the torque tracking is achieved. The torque hysteresis control strategies are discussed in detail [14]. The estimation of total torque adopts the look-up table method. The relationship of current, rotor position and torque are obtained by experimental data. Relation map between torque, current and rotor position is described in Figure 2.

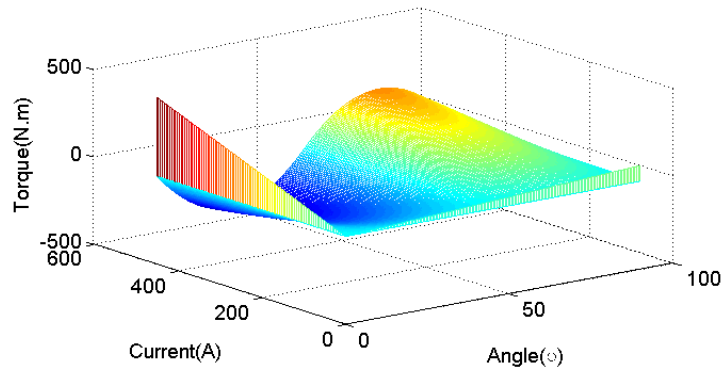


FIGURE 2. Relation map between torque, phase current and rotor position

4. The Simulation and Comparison Studies. In this section, the simulations are carried out in MATLAB to validate the proposed ITSMC for SRM speed control. In addition, performance comparisons between the proposed controller and traditional PI controller under the same conditions are conducted to assess the correctness and robustness of the proposed control scheme. The parameters of the simulation model of SRM drive are listed in Table 1.

TABLE 1. Parameters of the simulation model of SRM drive

Parameters	Value	Parameters	Value
Phase	3	Stator resistance	0.05Ω
Stator/Rotor pole numbers	6/4	Moment of inertia	$0.05\text{kg}\cdot\text{m}^2$
Rated power	60kw	Viscous friction	$0.02\text{N}\cdot\text{m}\cdot\text{s}$
Maximum current	450A	Aligned	23.6mH
Maximum flux linkage	0.486Wb	Unaligned	0.67mH

To confirm the advancement of proposed control strategy and the robustness against external load disturbance, some simulations were done.

First, to verify the effectiveness of the designed load torque observer, two changes of load torque: sudden increasing load T_L : $10\text{N}\cdot\text{m} \rightarrow 50\text{N}\cdot\text{m}$ and sudden dumping load T_L : $50\text{N}\cdot\text{m} \rightarrow 10\text{N}\cdot\text{m}$ were exerted. Estimated load torque of the load disturbance observer and load torque command are shown in Figure 3. The dashed line and the solid line represent the load torque command and the estimated load torque, respectively. It can be observed that the load disturbance observer can estimate the disturbance exactly and quickly.

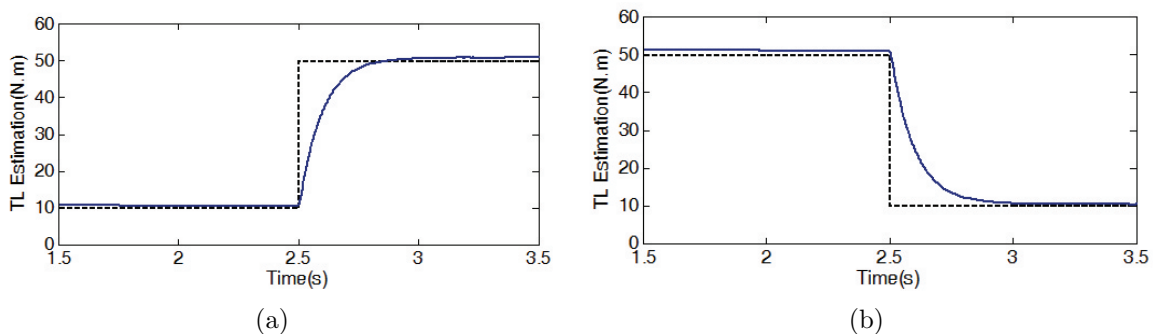


FIGURE 3. Observed load torque: (a) sudden increasing load, (b) sudden dumping load

Second, comparison studies are carried out between the proposed controller and traditional PI controller to confirm the wide range speed regulation capability of the proposed controller. The parameters (k_p and k_i) of the traditional PI speed controller were tuned to achieve satisfactory performance at a motor speed of 1500rpm with external load $T_L = 10\text{N}\cdot\text{m}$. The tuned k_p and k_i were 1 and 10, respectively. The simulations were implemented to regulate the SRM at different speed commands (100r/min and 1500r/min) with external load $T_L = 10\text{N}\cdot\text{m}$. The speed commands 100r/min and 1500r/min in this study were set for with 100r/min/s and 1500r/min/s slope, respectively. Figure 4(a) shows the simulation results for the proposed controller at 100r/min. Figure 4(b) illustrates the results for the traditional PI controller at 100r/min. As shown in Figure 4(a), the maximum transient speed error of the proposed controller is less than 0.5r/min. In

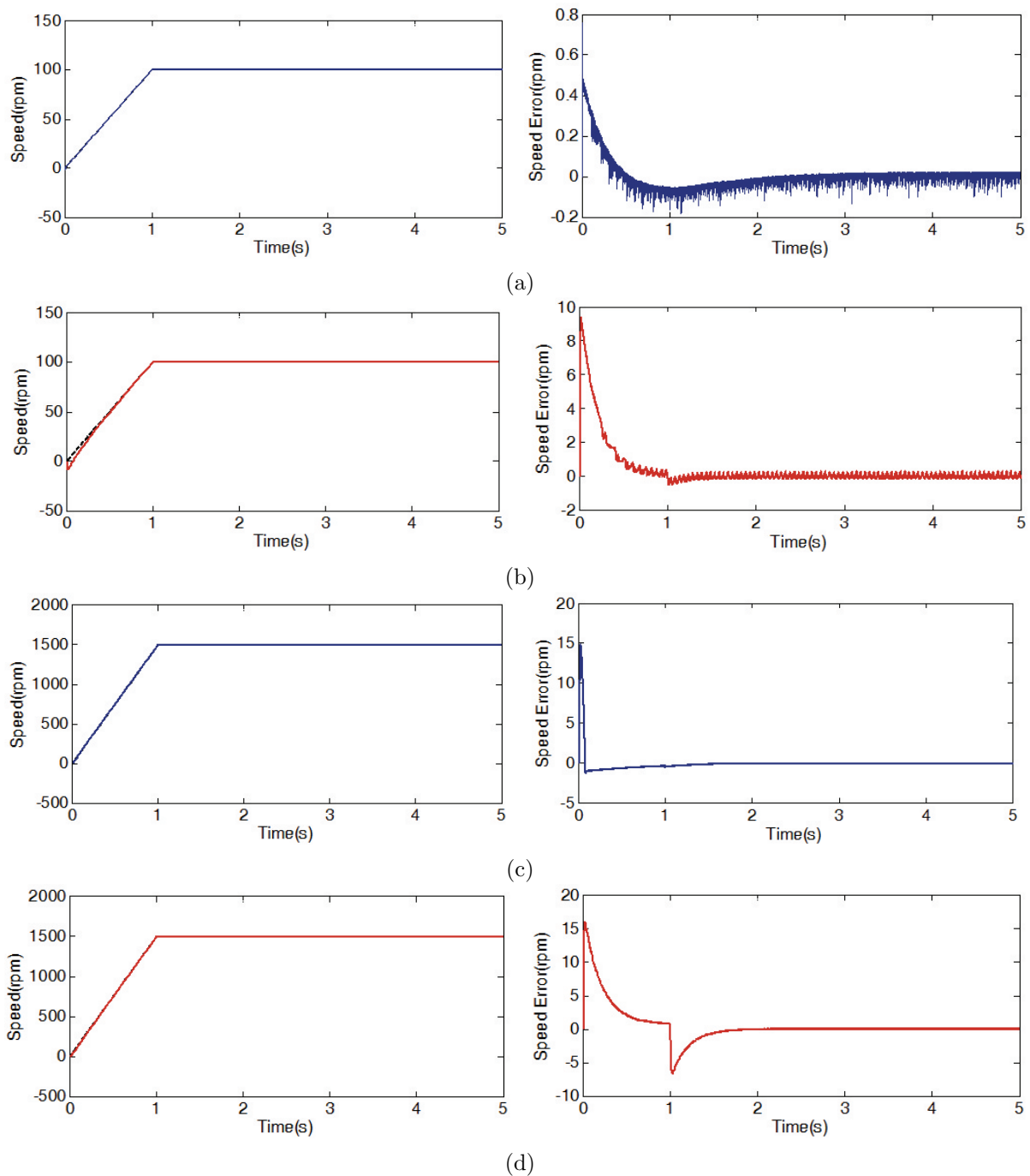


FIGURE 4. Speed responses under different speed commands: (a) ITSMC: 100r/min, (b) PI: 100r/min, (c) ITSMC: 1500r/min, (d) PI: 1500r/min

Figure 4(b), however, the maximum transient speed error of traditional PI controller is approximately 9.6r/min. Figures 4(c) and 4(d) plot the simulation results obtained using the proposed controller and traditional PI controller at 1500r/min reference speed. As shown in Figure 4(c), the maximum transient speed error of the proposed controller is less than 15r/min. In Figure 4(d), however, the maximum transient speed error of traditional PI controller is approximately 16r/min and speed response has a larger overshoot.

Finally, to confirm the robustness against the external load of the proposed controller, the following comparison simulations between proposed controller and PI controller were carried out at speed command 1500r/min. The proposed controller was started with external load $T_L = 10\text{N}\cdot\text{m}$, and an external load disturbance $T_L = 50\text{N}\cdot\text{m}$ was applied at 2.5s when the control system was in the steady state. Under the same conditions, the simulation of traditional PI controller is carried out. In Figure 5, the solid line and the dashed line represent the simulation results of the proposed controller and traditional PI controller, respectively. It can be observed that the speed fluctuations of the proposed controller are limited to less than 2r/min and recovers quickly. However, the speed dip of the traditional PI controller is approximately 35r/min and the actual speed recovers the setting speed after about 0.5s. This result reveals that the proposed controller has the good load disturbance rejection ability.

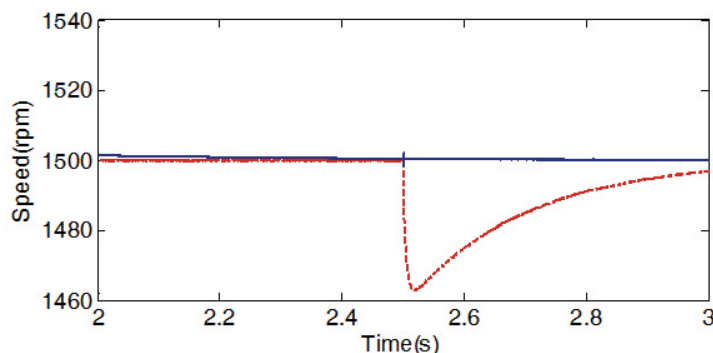


FIGURE 5. Speed response when the load is suddenly increased

5. Conclusions. This paper develops an ITSMC for the SRM drive system. The SRM drive system adopts the speed and torque double closed loop control. The integral term and time-varying term are introduced into sliding surface to enhance the speed control accuracy of the SRM drive system and to improve the convergence speed of the sliding surface. One load disturbance observer is designed to estimate system load torque and the observed load torque is integrated into the design of the sliding mode controller, which can better suppress the chattering of the controller. Simulation results show that the proposed approach can achieve accurate and fast speed regulation in the face of large external disturbances. The further research direction is expected to develop a high dynamic four quadrant SRM drive system based on DITC.

Acknowledgments. This work is supported by the Natural Science Foundation of Liaoning Province of China under Grant 2015020022, Fundamental Research Funds for the Central Universities under Grants 3132014321, and 3132016312. The authors would like to thank the reviewers for their helpful comments and suggestions, which have helped us to improve the presentation.

REFERENCES

- [1] Y. Sozer, I. Husain and D. A. Torrey, Guidance in selecting advanced control techniques for switched reluctance machine drives in emerging applications, *IEEE Trans. Industry Applications*, vol.51, no.6, pp.4505-4514, 2015.

- [2] K. Vijayakumar, R. Karthikeyan, S. Paramasivam et al., Switched reluctance motor modeling, design, simulation, and analysis: A comprehensive review, *IEEE Trans. Magnetics*, vol.44, no.12, pp.4605-4617, 2008.
- [3] M. I. Spong, R. Marino, S. M. Peresada et al., Feedback linearizing control of switched reluctance motors, *IEEE Trans. Automatic Control*, vol.32, no.5, pp.371-379, 1987.
- [4] C. Chen and T. Liu, Nonlinear controller design for switched reluctance drive systems, *IEEE Trans. Aerospace and Electronic Systems*, vol.39, no.4, pp.1429-1440, 2003.
- [5] X. Li and P. Shamsi, Inductance surface learning for model predictive current control of switched reluctance motors, *IEEE Trans. Transportation Electrification*, vol.1, no.3, pp.287-297, 2015.
- [6] C. L. Tseng, S. Y. Wang, S. C. Chien et al., Development of a self-tuning TSK-fuzzy speed control strategy for switched reluctance motor, *IEEE Trans. Power Electronics*, vol.27, no.4, pp.2141-2152, 2012.
- [7] C. A. Hudson, N. S. Lobo and R. Krishnan, Sensorless control of single switch-based switched reluctance motor drive using neural network, *IEEE Trans. Industrial Electronics*, vol.55, no.1, pp.321-329, 2008.
- [8] S. Rafael, P. J. Branco and A. J. Pires, Sliding mode angular position control for an 8/6 switched reluctance machine: Theoretical concept, design and experimental results, *Electric Power Systems Research*, vol.129, pp.62-74, 2015.
- [9] J. Deng, Q. H. Zhan and J. B. Sun, Speed control of switched reluctance motor using sliding mode variable structure control, *Micromotors*, vol.39, no.7, pp.1-4, 2005.
- [10] Y. J. Li, Z. W. Xu and X. Peng, The hybrid control of SRM based on sliding-mode variable structure control with integral action and neural network compensation, *Electric Machines and Control*, vol.15, no.1, pp.33-37, 2011.
- [11] Y. Cheng and H. Lin, Nonsingular fast terminal sliding mode positioning control in switched reluctance motor, *Electric Machines and Control*, vol.16, no.9, pp.78-82, 2012.
- [12] Z. Chen, J. Deng and X. D. Liu, An integral and exponential time-varying sliding mode control of permanent magnet synchronous motors, *Transactions of China Electrotechnical Society*, vol.26, no.6, pp.56-61, 2011.
- [13] S. S. Hu, *Automatic Control Theory*, Science Press, Beijing, 2007.
- [14] R. B. Inderka and R. W. De Doncker, DITC-Direct instantaneous torque control of switched reluctance drives, *IEEE Trans. Industry Applications*, vol.39, no.4, pp.1046-1051, 2003.